



The Thermochemical Deposition Approach was used to Manufacture a Lead Sulphide Composite Membrane, which exhibits Optical and Synthetic Properties

Atyaf Sarhan Farhan Alrubaie

Basic Sciences Branch, dentistry collage, AL-Qadisiyah University, Iraq, atyaf.s.farhan@qu.edu.iq

Abstract

This study involved the preparation of thin films of lead sulphide compound with three different thicknesses (150, 250, and 350 Nm) using pure materials of lead sulphate compounds, lead nitrate solution, and thiourea solution. The films were created through thermochemical deposition at a temperature of 623 K. Laboratory tests were conducted to determine the characteristics of the membranes, including the crystalline nature derived from lead sulphide and the cubic type with a diffraction pattern (200). Additionally, the membranes were analysed using an atomic force microscope, which revealed a decrease in the average square root and surface roughness. The findings demonstrated a positive correlation between the thickness of the lead sulphide membrane and the optical energy gap. This research aimed to assist researchers in the field of thin films by providing insights into the crystalline properties of lead sulphide membranes. These membranes hold significant value in scientific research, reagent applications, and the production of solar cells.

Keywords: Lead sulfide membranes , Optical energy gap , Thermochemical deposition

1. Introduction

Physics has deeply influenced numerous facets of daily existence, playing a crucial role in driving scientific and technological progress throughout history. The manufacturing of thin films is a significant application of physics that has been essential in advancing the knowledge of semiconductors ⁽¹⁾. Thin films are comprised of one or more layers of certain materials, with thicknesses that typically range from tens of nanometers to a few micrometers ⁽²⁾. The properties of these materials have intrigued physicists since the late 17th century. Extensive empirical scientific research has been conducted in this field, specifically investigating the practical aspects of thin films. Multiple semiconductors, such as selenium and silicon ⁽³⁾, have been employed in this field. Lead sulphide is a semiconductor material that has high optical conductivity specifically for infrared photons with long wavelengths. Lead sulphide is a semiconductor material that exhibits exceptional optical conductivity properties for infrared photons with extended wavelengths. Visible light, which falls within the wavelength range of 300-800 nanometers, is widely employed at normal ambient temperature for cell formation. The optical conductivity is employed in both military and civilian contexts. Through the analysis of the crystal structure and lattice dimensions of materials, we may determine the crystalline properties of matter, such as the size and density of atoms. Lead sulphide (PbS) is a crystalline compound that has a crystal structure resembling that of sodium chloride (NaCl), as seen in Figure (1). It consists of two groups, namely VI and IV.

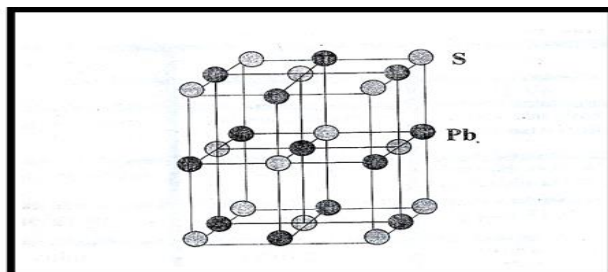


Figure (1) FCC crystal structure of the compound (PbS) ⁽⁸⁾

This indicates that PBS has a face-centered cubic (FCC) lattice structure with a lattice constant of $a=5.94 \text{ \AA}$. In this study, thin films of the PBS compound will be fabricated using the thermochemical deposition method. This method involves depositing a solution of the material onto heated substrates at a specific temperature, which leads to a thermochemical reaction between the substance's atoms and the heated base, resulting in the formation of a thin membrane. The membranes produced using this method possess favourable properties that make them suitable for utilisation in solar cell applications and reagents, as well as for investigating various physical attributes. The pioneering researchers (Hnger and Hottel) in 1959 were the first to employ this technique, successfully fabricating a black copper membrane on an aluminium substrate. This approach is distinguished by its simplicity and cost-effectiveness in using devices. It can be employed under typical weather circumstances and allows for the creation of membranes using materials with high melting points. Additionally, the method enables the preparation of membranes with excellent uniformity and wide surface areas. This process is widely regarded as a convenient technique for manufacturing membranes made of oxides and sulphates of various materials.

2. Experimental Part

Preparation of membranes

Lead sulfide (PbS)

The compound (PbS) is a polar semiconductor with a mixed chemical bonding nature. It exhibits both ionic and covalent bonds, with the ionic component dominating over the covalent component. This indicates that the compound (PbS) shares structural similarities with ionic compounds. In 1956, Krebs proposed a bonding system for compounds of the PbS type that shows the presence of both ionic and covalent bonds. In a pure ionic compound, Pb^{+2} ions have three empty levels in the P-state, while S ions have one pair of electrons in the S-state and three pairs of electrons in the P-state. As a result, each sulphur ion is surrounded by six lead ions in an octahedral shape, and each lead ion is surrounded by six sulphur ions⁽¹¹⁾.

Table(1) shows the physical and chemical properties of PbS material ^(12,13,14) .

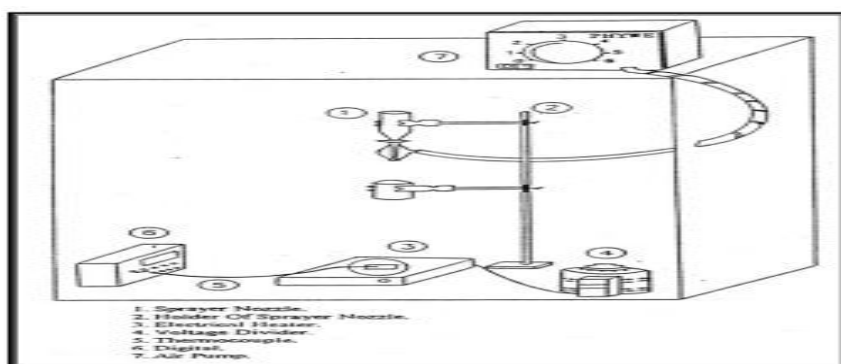
Properties	PbS
Formula Weight gm/mol.	239.25
Density gm/cm ³	7.5
Melting point °C	1114
Boiling point °C	-
Coefficient of & linear Expansion at 300k °C ⁻¹	2.03*10 ⁻⁵
Energy Gap at 300 K(eV)	0.41
Gap Transition	Direct
Electron Affinity (eV)	4.21
Mobility of Electrons at 300K (cm ² /V.Sec)	500
Mobility of Holes at 300K (cm ² /V.Sec)	600
Effective Mass Electron	0.25
Effective Mass Holes	0.25
Work function at 300K (eV)	4.53
Dielectric Constant (Relative)	17.0
Lattice Constant (Å)	5.936
Colour	Black

Thermochemical deposition system:

The system comprises multiple uncomplicated components, as depicted in Figure (2) ⁽¹²⁾. Thin films of various chemicals and bases can be obtained using this method. They have been utilised to create a thin membrane of the research material (PbS) on directed Silicon bases (111). The bases have been utilised to fabricate a thin PbS compound membrane on Silicon bases⁽¹³⁾, and the system comprises the following devices:

1. atomizer
2. aerosol dispenser holder
3. device that converts electrical energy into heat
4. Voltage divider refers to a circuit that divides the input voltage into smaller output voltages based on the ratio of resistances in the circuit.
5. Dual thermocouple refers to a setup that involves two thermocouples, which are temperature sensors that generate a voltage proportional to the temperature difference between their junctions.
6. pneumatic pump

Figure(2) shows the thermochemical deposition system



X-ray diffraction:

X-ray photon diffraction is a significant technique used to get precise and comprehensive data regarding the crystalline structure of solid materials ⁽¹⁴⁾. The optical characteristics of the films were acquired using an X-ray diffraction apparatus.

Target: Cu-K α ,
 wavelength: 1.5406 (Å)
 Voltage: 40 (kV),
 current: 30 (mA)

Atomic force microscope (AFM)

Using this method, one may determine the surface topography, quantify the roughness, and calculate the roughness coefficient ⁽¹⁵⁾.

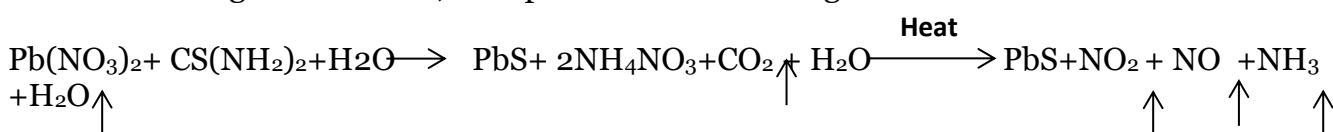
field scanning electron microscope (SEM):

Is a type of microscope that uses electrons to scan and analyse the surface of a sample. The FEI FESEM NanoSEM Nova 450 scanning electron microscope is a cutting-edge instrument with strategic significance. This device is regarded as a sophisticated instrument in the realm of nanotechnology research and has extensive applications. This gadget has a magnification capability over two million times and can achieve accuracy within a few nanometers. Additionally, it utilises EDX technology to accurately analyse the proportions of material constituents. The equipment is situated at the Department of Physics within the Faculty of Science at the University of Basra.

3. Results and discussion

Preparation of membranes:

A solution was prepared by dissolving 4.311 g of pure lead nitrate (99.9% purity, Pb(NO₃)₂) in 50 ml of distilled water for 17 minutes. The lead nitrate was obtained with a molar concentration of (0.1). To remove impurities present in the laboratory atmosphere during the preparation process, the resulting colourless solution was filtered using filter paper. This solution was used to obtain lead sulphide membranes in combination with thiourea (CS(NH₂)₂). A highly pure thiourea compound with a purity of 99.9% and a concentration of 0.1 molar was utilised. To dissolve 8.611 of these compounds, 50 ml of distilled water was employed. The dissolution process was completed within 15 minutes, resulting in a colourless solution. Subsequently, the solution was filtered using the same method as lead nitrate. A sensitive scale with high precision was employed to measure the weight of the utilised materials. The Malol obtained from lead nitrate was combined with the resultant thiourea solution. The reaction resulted in the release of carbon dioxide, while simultaneously maintaining the solubility of lead sulphide and ammonium nitrate in water. Ammonium nitrate undergoes decomposition when exposed to precipitation, resulting in the release of various gases including nitrogen dioxide, a poisonous gas, nitrous gas, and ammonia gas. The water undergoes evaporation, leading to the deposition of a lead sulphide membrane on the surface of a glass substrate, as depicted in the following reaction.:



4. Conclusion

The findings from the X-ray diffraction analysis of PbS membranes are as follows:

The images clearly demonstrate that the X-ray diffraction results of thin (PbS) membranes, which were created using the thermochemical deposition method at varying temperatures and thicknesses, suggest the presence of a polycrystalline structure. This finding is consistent with the researcher's observations ⁽¹⁶⁾. The structure is cubic, which aligns with the findings of the researcher ⁽¹⁷⁾. Upon analysing the practical values using the ASTM CARDS American standard Testing Metal, it was observed that the reflection peaks of (PbS) tables are (111) and (200). These peaks indicate a high degree of crystallisation, with a particularly strong and sharp peak in the (200) direction. Additionally, there is evidence of swelling and an increase in thickness. This information can be further corroborated by referring to Figure (3). A minor peak is observed at a 2θ value of 27.25 degrees for the (111) plane. It is noticed that the peak in X-ray diffraction of these membranes grows with an increase in temperature, thickness, and shape. The patterns were observed at 2θ angles ranging from 32 to 37 degrees. At a thickness of 350 nanometers, there is a prominent peak attributed to lead (Pb) that is observed at high temperatures. This peak may be caused by the separation of the lead sulphide (PbS) layer at elevated temperatures. At lower temperatures, the effect of this separation is less pronounced. The presence of this peak can be attributed to the regularity of the crystal structure, which aligns with the findings of researcher ⁽¹⁸⁾.

Figure (3) x-ray diffraction diagram of pure PbS membranes with various thickness

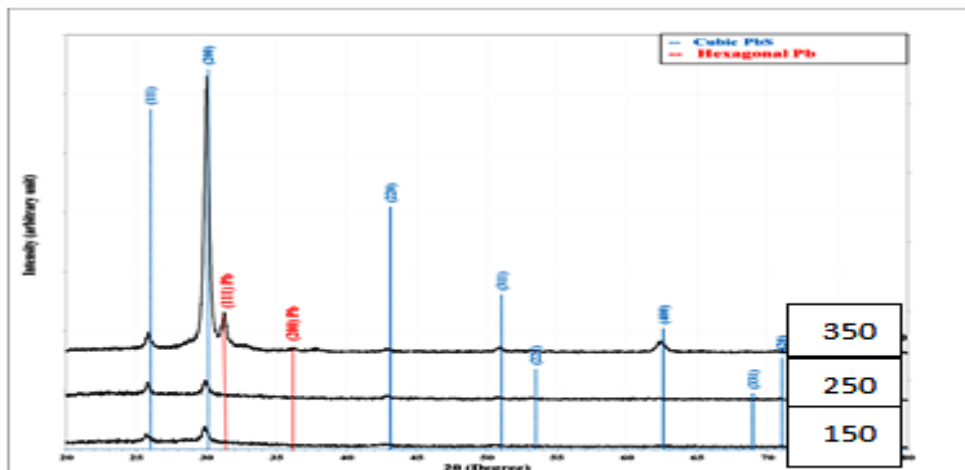


Table (2): shows the values of the distance between the Crystal levels and the locations of the peaks and the Miller coefficients for thin (PbS) membranes prepared with different mixing ratios

sample	2θ (Degree)	d_{hkl} Experiment (Angstrom)	d_{hkl} standard (Angstrom)	FWHM (Degree)	Crystal size (Nanometer)	Hkl	Phase	card Number
150	25.68	3.46	3.42	0.28	28.4	(111)	Cub. PbS	96-901-3403
	29.89	2.99	2.96	0.50	16.1	(200)	Cub. PbS	96-901-3403
250	25.79	3.45	3.42	0.37	21.8	(111)	Cub. PbS	96-901-3403
	29.90	2.97	2.96	0.44	18.1	(200)	Cub. PbS	96-901-3403
	42.85	2.10	2.09	0.37	22.9	(220)	Cub. PbS	96-901-3403
350	25.88	3.43	3.42	0.40	20.3	(111)	Cub. PbS	96-901-3403
	30.03	2.95	2.96	0.42	20.1	(200)	Cub. PbS	96-901-3403
	31.25	2.85	2.85	0.37	22.1	(111)	Hex. Pb	96-900-8478
	36.22	2.47	2.47	0.31	26.5	(200)	Hex. Pb	96-900-8478
	42.99	2.10	2.09	0.37	22.9	(220)	Cub. PbS	96-901-3403

Lattice constants (a_0 , c_0)

The lattice constants (a_0 , c_0) for all prepared membranes were calculated using the relation ⁽¹⁹⁾.

$$d_{hkl} = \frac{a}{\sqrt{h^2 + k^2 + l^2}}$$

Table (3) indicates that the lattice constants for thin PbS membranes match the values listed in the international card for the material. The lattice constant for the PbS compound is measured to be 3.792 Å.

Table (3) shows the value of the lattice constants of thin PBS membranes with the values found in the international card of the material

Sample	Pbs	Pbs	Pbs
	150 Nanometer	250 Nanometer	350 Nanometer
hkl	(200)	(200)	(200)
2θ (deg)	29.89	29.90	30.03
d_{hkl} (Å)	2.99	2.97	2.95
FWHM (deg)	0.50	0.44	0.42
Lattice constant (a_0) (Å) $a^{\circ}=b^{\circ}=c^{\circ}$	5.95	5.99	5.97
D (Nanometer)	16.1	18.1	20.1

Results of atomic force microscope examinations(AFM) and Crystal volume (D):

The Crystal volume of all prepared membranes and the highest Vertex has been calculated using the Scherrer equation (Scherrer's Formula) according to the relationship ⁽¹⁹⁾

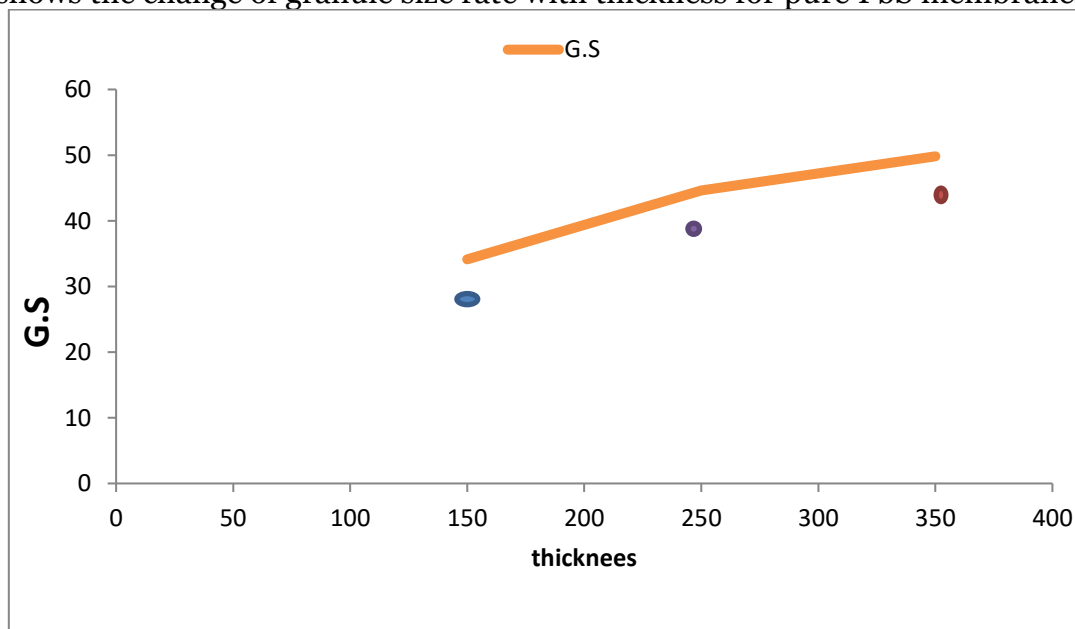
$$D_{ave} = \frac{0.9 \lambda}{B \cos \theta}$$

The results indicate that the average granular size of PBS membranes increases with swelling thickness, specifically with higher swelling temperatures. This finding is in line with previous studies (20). Additionally, the largest crystal size of the PBS compound is 20.1 nanometers at a thickness of 350 nanometers. The explanation for this phenomenon is the rise in temperature, which results in granulation. This suggests an improvement in the regularity of the membranes, an enhancement in the crystallisation process, and a reduction in crystal flaws.

Table (4): values of the average Grain Size rate for thin PbS membranes.

Sample	PbS150nm	PbS250nm	PbS350nm
Average Grain Size(nm)	34.13	44.62	49.82

Figure (4) shows the change of granule size rate with thickness for pure PbS membranes



The topography of the precipitating materials of PbS membranes, prepared using the thin thermochemical deposition method, was analysed using the atomic force microscope (AFM). The AFM provided high-resolution images and accurate statistical values for the average grain size and distribution. Figure (5) displays the AFM images and results of the thin films (PbS), showing the granule size distribution of the prepared membranes. Table (4) presents the values for surface

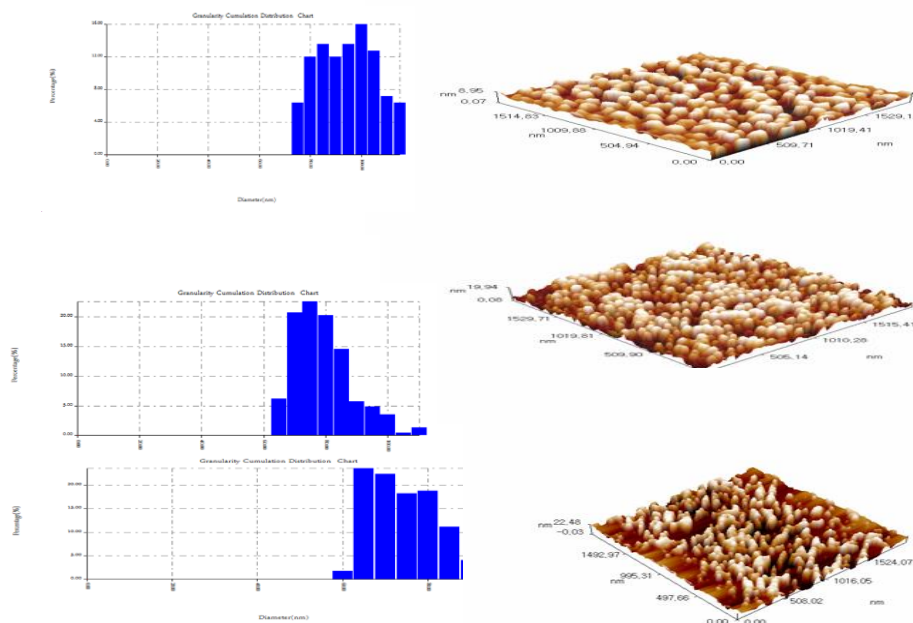
roughness, root mean square (RMS) of the average surface roughness, and the average grain size for the PbS membranes.

From the table, it is evident that the highest values for both the surface roughness and the square root of the mean roughness of the membrane are observed for (PbS350). This indicates that increasing the base temperature leads to an increase in both the surface roughness and the square root of the mean roughness. Additionally, it can be observed from the table that the grain size values exhibit random fluctuations. The results confirm that an increase in the size of the crystals and a reduction in the granular boundaries are directly proportional to the square root of the square of the mean roughness. These findings align with the results obtained from X-ray diffraction (XRD), which also indicate an increase in crystal size with an increase in the degree of thickness. The researcher's observations are in agreement with these results ⁽¹⁶⁾.

Table (5): surface roughness values and the square of the mean roughness RMS and the grain size rate of pure PbS membranes

Sample	Surface roughness (nm)	RMS (nm)	Average Grain Size (nm)
PbS150nm	3.15	3.5	72.40
PbS250nm	5.96	6.73	78.83
PbS350nm	6.96	7.5	94.01

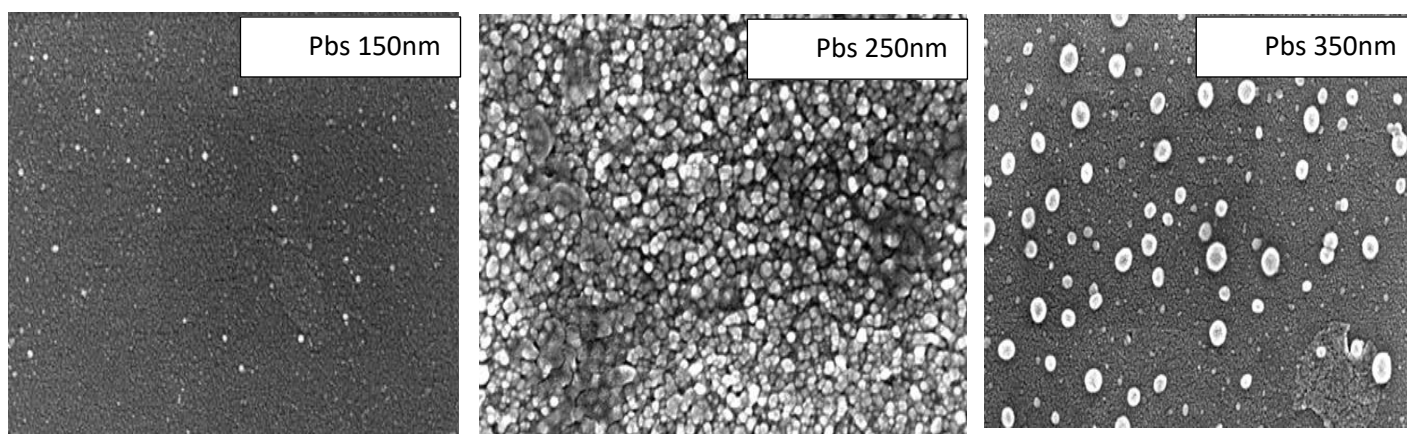
Figure (5): AFM images and results of thin PbS membranes prepared with different thickness.



Results of field-emitting scanning electron microscope examinations:

The surface topography of the precipitating materials in all prepared membranes was examined using a Field Emission Scanning Electron Microscope (FESEM). This device provided high magnification and resolution images of the surfaces. Figure 6 displays the FESEM images of thin PbS membranes. It is evident from the figure that the surface structure of the membranes, specifically the PbS150Nanometer and PbS250Nanometer membranes, consists of regularly arranged nanostructured forms. Regarding the membrane (PbS350Nanometer), it is observed that it is a nanostructure composed of aligned and stacked units. These units are made up of numerous cohesive grains that have grown due to elevated temperatures, resulting in their aggregation in this particular configuration.

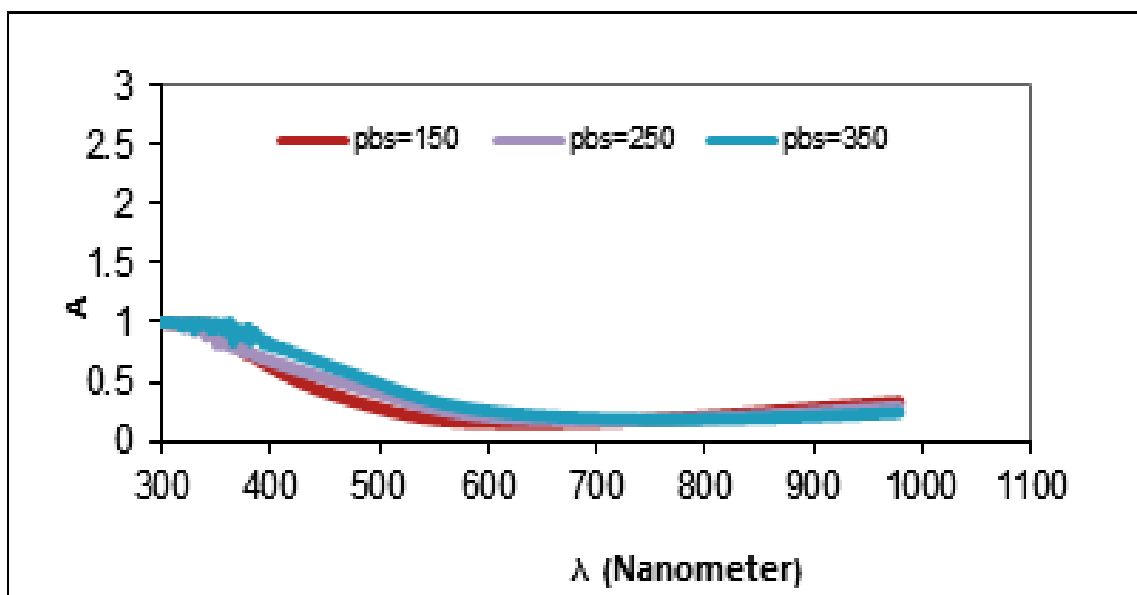
Figure (6): Field-Emitting Scanning Electron Microscope images of thin PbS membranes.



Absorptivity:

The study focused on measuring the absorptivity of a compound (PbS) in relation to different wavelengths. By analysing the absorption spectrum, various optical parameters were determined. The assessment was conducted within the nanometer wavelength range of 300-1100. The results, shown in Figure (7), indicated that the absorption spectrum of the compound PbS increases as the thickness of the deposited material increases. This finding aligns with the previous research conducted by the researcher (16). It is evident that the absorption spectrum will amplify as the thickness of the swelling increases, particularly within the wavelength range of 600 to 1000 nanometers. Specifically, we detect an augmentation in the absorption spectrum at a thickness level of 150 nanometers, within the wavelength range of 650 to 1100 nanometers.

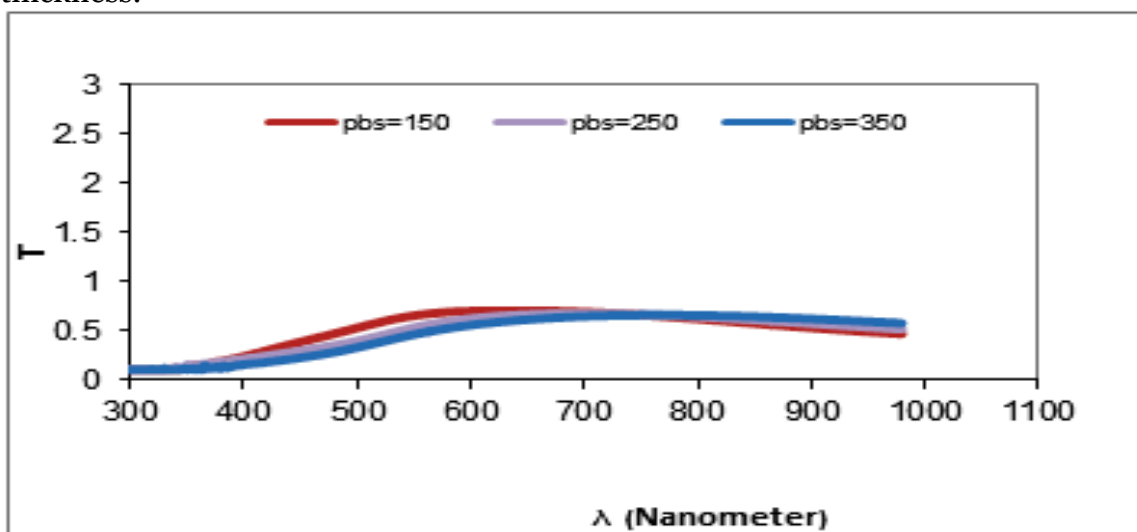
Figure (7) curves the absorption spectra as a function of the wavelength of pure PbS samples with different thickness.



Permeability:

The UV-VIS measurements of all PbS membranes indicate that the transmittance spectrum decreases as the wavelength of swelling increases. The lack of permeability is attributed to an increase in the percentage of PbS, which is caused by larger crystal size and a decrease in crystal defects due to an increase in lead ions. This finding aligns with the observations made by the researcher (16), where a decrease in transmittance is observed at a level of 150 nanometers during the wavelength range of 650 to 1100 nanometers.

Figure (8) curved transmittance Spectra as a function of wavelength for pure PbS samples with different thickness.



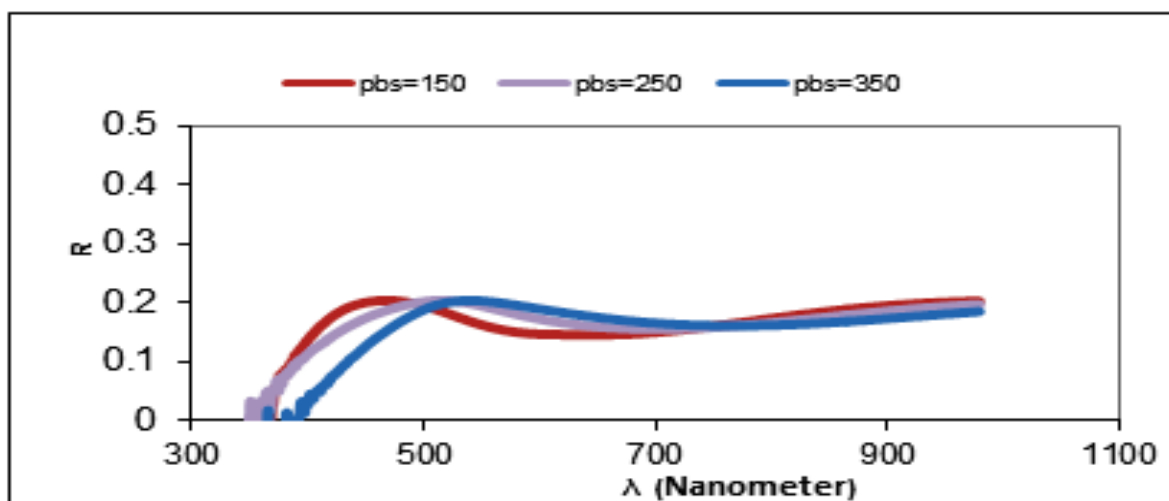
Reflexivity:

Reflectivity as a function of wavelength was calculated approximately from the spectrum of absorbance and permeability and by the law of conservation of energy by the equation⁽¹⁷⁾

$$R = 1 - T - A$$

Figure (9) displays the reflectivity. The reflectivity curves generally show an increase in reflectivity values across the wavelength range. The highest reflectivity is observed at a thickness of PbS₃₅₀, with an increase of 0.17. Between the wavelength range of 300-750 Nanometers, the reflectivity of PbS₁₅₀ Nanometer thickness starts to increase. During this range, the reflectivity for a thickness of 150 Nanometers is 0.037, while for a thickness of 250 Nanometers it is 0.035.

Figure (9) the optical reflectivity changes as a function of the energy of the wavelength of the composition PbS and in different proportions



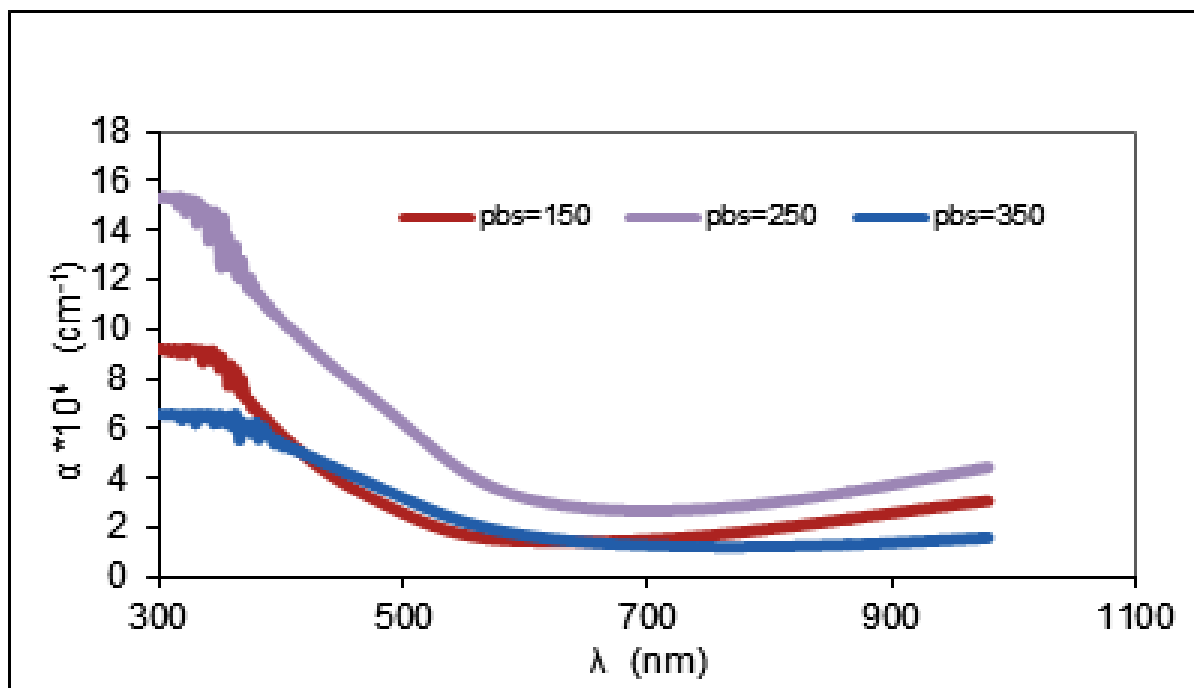
Absorption coefficient :

The absorption coefficient was calculated from the equation

$$\alpha = 2.303 (A/t)$$

When studying the absorption and permeability spectrum of PbS membranes, we noticed a decrease in the absorption coefficient as the thickness of the membranes increased. This decrease in absorption coefficient may be attributed to the creation of energy levels within the energy gap, resulting in the absorption of low-energy photons. This finding aligns with the results reported by researcher (16). Additionally, we observed a significant increase in the absorption coefficient of fish (PbS₃₅₀Nanometer) within the wavelength range of 300-1100 Nanometers.

Figure (10) the change of the absorption coefficient as a function of the wavelength of pure non-membrane PbS with different thickness .



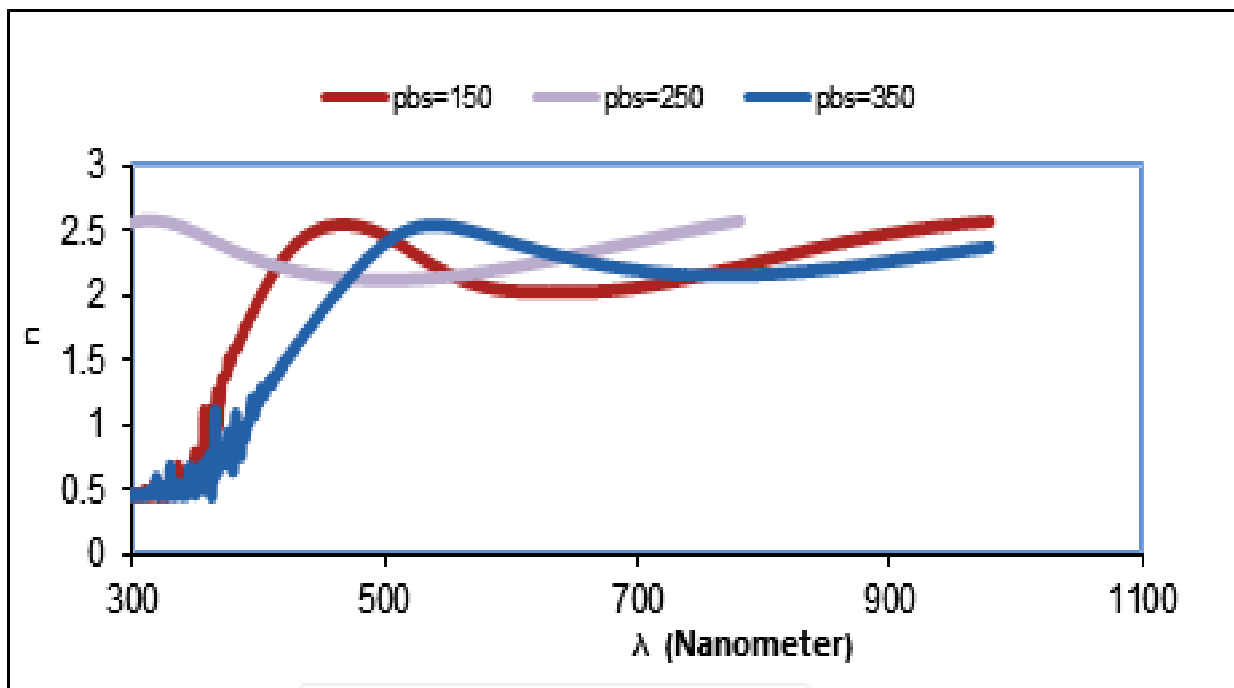
Refractive index:

The refractive index (n) is the ratio between the speed of light in a vacuum to its speed inside the material, and the refractive index depends on several factors, including the type of material and its composition . The refractive index was calculated using the relation

$$n_o = \left(\left\{ \frac{(1+R)}{(1-R)} \right\}^2 - (K^2 + 1) \right)^{1/2} + \left\{ \frac{(1+R)}{(1-R)} \right\}$$

Figure (11), which shows the change in refractive index with wavelength and for different thicknesses of the compound (PbS) through the pattern, we notice an increase in the refractive index by swelling thickness and the refractive index of the compound (PbS) is within the range of (0.5-2.5).

Figure (11) refractive index changes as a function of wavelength (membrane PbS) and with different thickness .



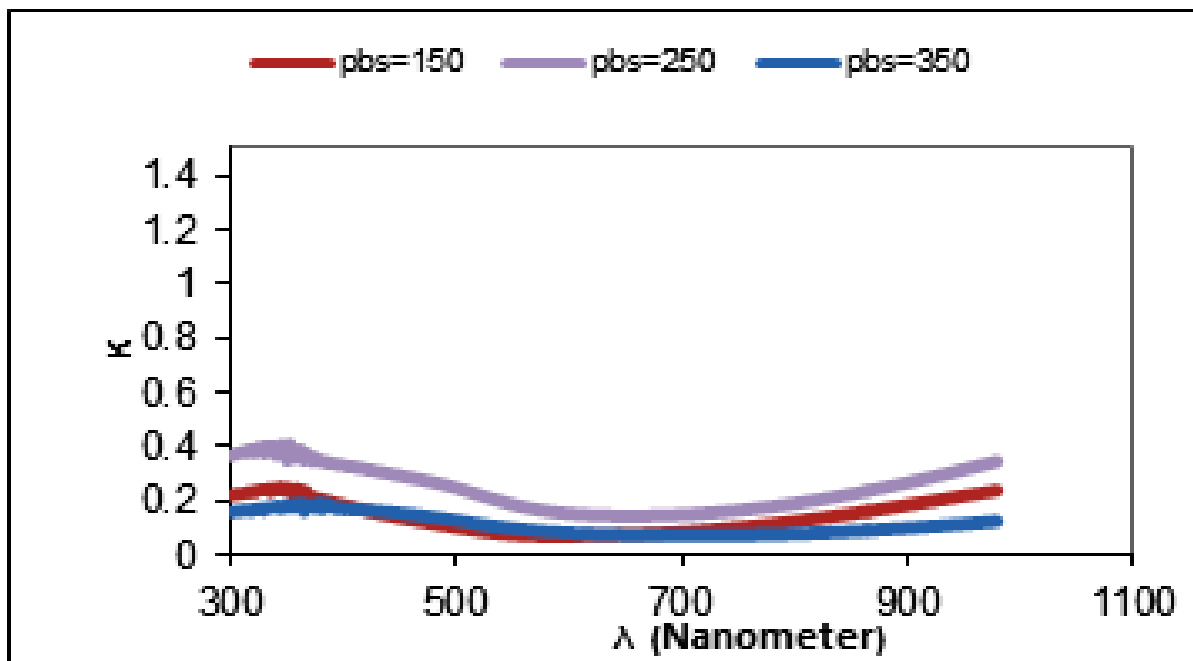
Extinction Coefficient (k^o) :

The coefficient of inertia represents the value of the inertia or diminution of the electromagnetic wave inside the membrane material and the coefficient of inertia was calculated according to the relationship⁽¹⁷⁾ :

$$K = \alpha\lambda / 4\pi$$

And as in Figure (12), which shows the change of the coefficient of inertia with the wavelength of the compound (PbS), we note from the figure that the coefficient of inertia will also diminution with swelling thickness and we notice during the wavelength between (550-1100Nanometer) we notice an increase in the coefficient of inertia and therefore during the wavelength (550-110Nanometer) the coefficient of inertia will increase with swelling thickness

Figure (12) the change of the coefficient of inertia as a function of the wavelength of non-membrane PbS with different thickness



Optical energy gap (E_{g}^{opt}) the Optical Energy Gap:

The optical energy gap was found by the equation ⁽¹⁷⁾

$$\alpha h\nu = B (h\nu - E_{g}^{opt})^{1/2}$$

The values of the optical energy gap (E_{g}^{opt}) of the membranes can be found by pattern a graph relationship between $(h\nu)^2$ and the Photon Energy, After that, the tangent of the curved part containing the primary absorption edge is drawn and by taking the extension of this tangent to cut the Photon Energy Axis (X-axis) at the point $((h\nu)^2=0)$, we obtain the value of the energy gap forbidden for the allowed direct transition, as shown in Figure (13), which shows the energy gap for the allowed direct transition of the compound to the compound (PbS) and the results showed an increase in the value of the found that the value of the E_{g}^{opt} of the PbS material in this transition is within the range (0.4-2.8) eV, where the energy gap of the vehicle is PbS=0.4 if infrared radiation is used. energy gap by swelling the thickness this is consistent with the researcher ⁽¹⁶⁾.

Figure (13) the value of the optical energy gap of the permissible direct membrane transitions PbS.

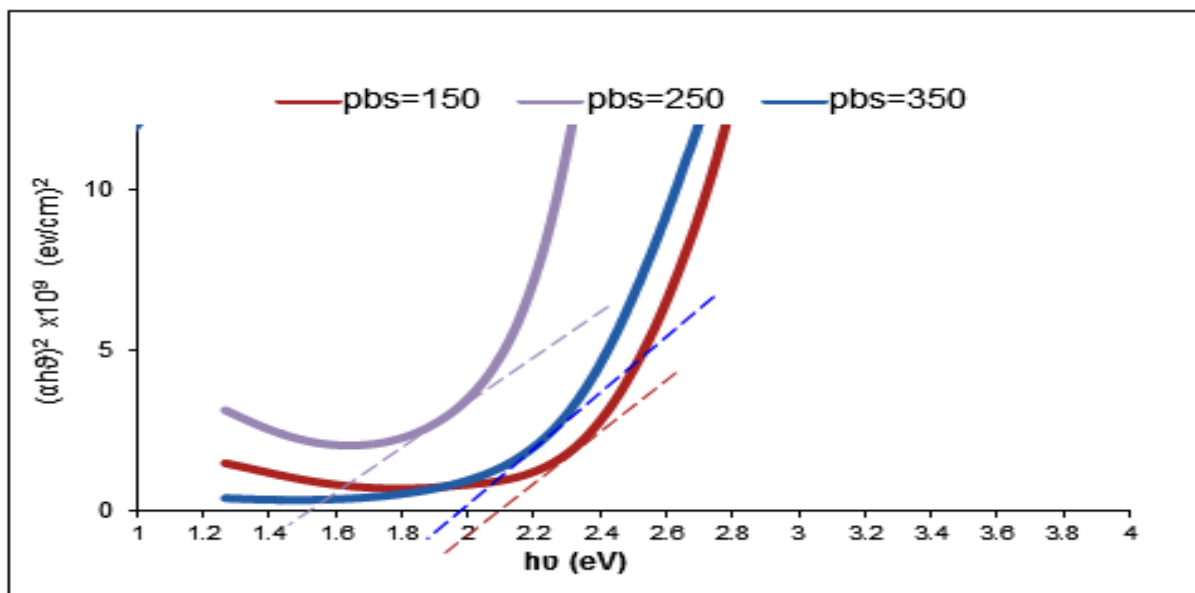


Table (6) shows the values of the permissible energy gap of the compound (PbS) prepared with different fish .

Sample	$E_{g^{opt}}$ (eV)
Pbs150Nanometer	2.1
Pbs250Nanometer	1.5
Pbs350Nanometer	1.9

References

- [1] رعد سعيد عبد الراوي "دراسة بعض الخصائص التركيبية والبصرية والكهربائية الغشبية الاننيمون واليزموث والتليريوم المرسبة بوضع مائل" اطروحة دكتوراه، الجامعة التكنولوجية، (2001).
- [2] بان يوسف حنا، "الصفات الضوئية الغشبية CdO, ZnO ولمزيجهما بنسب حجمية مختلفة"، رسالة ماجستير الجامعة المستنصرية . 1991
- [3] O. S. Heavens, "Thin film physics", Methum & Colted (1970).
- [4] L.Pintilie ,E.Pentia,I.Matei , J.Appl.Phys., Letters, Vol.4, No.73, P:547, (1998).
- [5] W.W.Scanlon, J.Phys.Chem.Solid, Vol.4, No.423, (1959).
- [6] P.J.Lin-Chung , J.Phys.Chem.Solids, Vol.2, No.31, (1970)
- [7] D.Dalven, Infrared phusico, Vol.4, No.41, (1969).
- [8] <http://www.Band Structure of PbS>, (2000).



- [9] H. G. Rashid," Design and optimization of thin films optical filters with applications in the visible and infrared regions ", Ph.D. thesis, Al-Mustansiriya University, (1996)
- [10] Y.U.L. Ravich B.A. Efimova, Semi-Conducting Lead Chalcogenides Plenum Press, New York, London, (1970)
- [11] H.Krebs, Acta Cryst., Vol.9, P:95, (1956).
- [12] L.Pintilie, E. Pentia , I. Matei , and I. Pintilie , "Journal of Applied Physics", Vol.91, [13] R.C. Weast and M.J. Astle "Hand Book of Chemistry and Physics", CRC Press, (1979). [14] N.N. Greenwood & A.Eraushaw in "Chemistry of The Elements , 2nd edition, Butter Worth, UK, (1997)
- [15] محمد امين سليمان ، احمد فؤاد باشا وشريف احمد خيرى ، فيزياء الجوامد ، مطبعة الفكر العربي , (2000)
- [16] C. Heidari, M. Rabani and B. Ramezanzadeh, "Applications of CuS- ZnS PN Junction for Photoelectrochemical Water Splitting", Int. J. Hydrogen Energ, Vol. 42, pp. (9545-9552), (2017).
- [17] PS. A. Tawfiq " A study of optical and electrical properties of the cadmium stannate material using the Co - Evaporation method " PH.D. Thesis , Al –Mustansiriya University, (1996) .
- [18] A. S. Fathima, N. Sivaguru and V. S. Kumar,"Investigation on Op-
- [19] Ptical Properties of CuS Thin Films by Chemical Bath Deposition ", IOSR- J. Appl. Phys, Vol. 4, pp. (13-16), (2016).
- [20] T. W. Edwards and Hicks, "Pump Application Engineering " Mc Graw – Hill ,Book Company, (1971)